Author Manuscript

Author Manuscript

Author Manuscript

Author Manuscript

HHS Public Access

Author manuscript

Biochem Cell Biol. Author manuscript; available in PMC 2022 November 10.

Published in final edited form as:

Biochem Cell Biol. 2017 June ; 95(3): 421–427. doi:10.1139/bcb-2015-0090.

Temporo-spacial microanatomical distribution of the murine sodium-dependent ascorbic acid transporters *Slc23a1* and *Slc23a2* in the kidney throughout development

Peter K. Eck,

University of Manitoba, Department of Human Nutritional Sciences, W569 Duff Roblin Building, 190 Dysart Road, University of Manitoba, Winnipeg, MB R3T 2N2, Canada; Molecular and Clinical Nutrition Section, Building 10, Room 4D52 MSC 1372, National Institutes of Health, Bethesda, MD 20892-1372, USA.

Christopher Corpe,

Molecular and Clinical Nutrition Section, Building 10, Room 4D52 MSC 1372, National Institutes of Health, Bethesda, MD 20892-1372, USA; Department of Nutrition and Dietetics, Diabetes & Nutritional Sciences Division, School of Medicine, King's College London, Room 3.114 Franklin-Wilkins Building, 150 Stamford Street, London SE1 9NH, UK.

Mark A. Levine

Molecular and Clinical Nutrition Section, Building 10, Room 4D52 MSC 1372, National Institutes of Health, Bethesda, MD 20892-1372, USA.

Abstract

The two membrane transporters Slc23a1 and Slc23a2 mediate ascorbic acid uptake into cells. We recently determined the key role of Slc23a1 in renal re-absorption of ascorbic acid in a knockout mouse model. However, the renal spatial and temporal expression patterns of murine *Slc23a1* and *Slc23a2* are not defined. This study utilizes database evidence combined with experimental confirmation via in-situ hybridization to define the spatial and temporal expression of *Slc23a1* in the murine kidney. *Slc23a1* is expressed in the early proximal tubule, but not in its precursors during embryonic development, and exclusive proximal tubular expression persists throughout the animal's lifetime. In contrast, *Slc23a2* is uniformly expressed in metabolic cell types such as stromal cells. The expression patterns appear to be conserved from rodent lineages to humans.

Résumé :

Les deux transporteurs membranaires Slc23a1 et Slc23a2 assurent la captation de l'acide ascorbique dans les cellules. Les auteurs ont récemment déterminé le rôle clé de Slc23a1 dans la réabsorption rénale d'acide ascorbique dans un modèle de souris knockout. Cependant, les patrons d'expression spatiaux et temporels de *Slc23a1* et *Slc23a2* chez la souris ne sont pas définis. Cette étude utilise des éléments probants issus de bases de données combinés à une confirmation expérimentale par hybridation *in situ* afin de définir l'expression spatiale et temporelle de *Slc23a1*

Corresponding author: Peter K. Eck (peter.eck@ad.umanitoba.ca).

Conflict of interest

The authors declare that they have no competing interest to disclose in association with this work.

Author Manuscript Author Manuscript Author Manuscript Author Manuscript

dans le rein de souris. *Slc23a1* est exprimé dans le tubule proximal précoce mais non chez ses précurseurs durant le développement embryonnaire, et l'expression exclusive dans le tubule proximal persiste durant toute la vie de l'animal. Par contre, *Slc23a2* est exprimé uniformément dans les types de cellules métaboliques comme les cellules stromales. Ces patrons d'expression semblent être conservés des lignages de rongeurs à l'humain. [Traduit par la Rédaction]

Keywords

Slc23a1; Slc23a2; kidney; murine; development

Mots-clés:

Slc23a1; Slc23a2; rein; souris; développement

Introduction

Ascorbic acid (ascorbate, vitamin C) is an indispensable metabolite essential for survival. Ascorbate cannot be synthesized in humans, owing to the loss of functional gulonolactone oxidase (EC 1.1.3.8), but is synthesized in murine species, such as mouse and rat (Nishikimi et al. 1988; Padayatty et al. 2003). The kidney is a central organ for ascorbic acid homeostasis. Slc23a1 plays a key role in ascorbate homeostasis and pharmacokinetics, as demonstrated by the facts that *Slc23a1*$^{-/-}$ knockout mice have very high urinary losses leading to low systemic concentrations (Corpe et al. 2010). Slc23a1 is known to mediate ascorbic acid uptake into epithelial cells of the small intestine, liver, and kidney (Maulén et al. 2003; Boyer et al. 2005; Lee et al. 2006; Luo et al. 2008; Varma et al. 2008), and is also expressed in some epithelia of the reproductive system and the brain (Tsukaguchi et al. 1999). Slc23a1 transports ascorbic acid with comparatively low affinity ($K_M \approx 250$ μmol/L) but high capacity, reflecting its role in intestinal absorption and renal re-absorption (Daruwala et al. 1999; Tsukaguchi et al. 1999). Compared with the wildtype controls, the *Slc23a1*$^{-/-}$ mouse has an up to 18-fold increase in fractional ascorbate excretion. The consequence is that ascorbate renal reabsorption is lost, resulting in low plasma and tissue concentrations and high perinatal loss of offspring (Corpe et al. 2010).

A second ascorbic acid transporter, *Slc23a2*, is found in almost all cell types, mediates ascorbic acid transport across cell membranes with high affinity ($K_M = 15$ μmol/L), and requires cations (Na^+, Ca^{2+}, or Mg^{2+}) for optimal activity (Daruwala et al. 1999; Tsukaguchi et al. 1999; Godoy et al. 2007). The global elimination of *Slc23a2* results in undetectable ascorbate tissue concentrations, and *Slc23a2*$^{-/-}$ mice die within minutes of birth (Sotiriou et al. 2002). Owing to its expression in a wide range of tissues, it is generally accepted that Slc23a2 is responsible for the ascorbate tissue accumulation needed for survival (Sotiriou et al. 2002).

Despite the importance of both sodium-dependent ascorbic acid transporters and the fact that both genes have been eliminated in mouse models, their spatial expression in defined anatomical compartments of the nephron and the temporal expression during embryonic development are not described for murine species. This study reports the temporal-spatial

Author Manuscript Author Manuscript Author Manuscript Author Manuscript

distribution of the murine *Slc23a1* and *Slc23a2* transcripts throughout kidney developmental stages by comparing in-situ hybridization (ISH), microarray data, and quantitative PCR data of nephron compartments.

Materials and methods

In-situ hybridizations

Organ samples—Samples were obtained from embryonic mice and adult rats as part of the animal protocols approved by the Eunice Kennedy Shriver National Institute of Child Health and Human Development and the National Institute of Diabetes and Digestive and Kidney Diseases Animal Care and Use Committees. Specimens were harvested, snap frozen in dry ice, and stored at −70 °C. Serial sections of 10 μm thickness were cut at −15 °C and thaw-mounted onto poly-L-lysine-coated slides for in-situ hybridization or immunohistochemistry.

Probes for hybridization and visualization—The human *SLC23A1* and *SLC23A2* complete coding sequences subcloned into pGEM-T Easy Vectors (Promega) were used to prepare RNA probes for in-situ hybridizations (Daruwala et al. 1999). The synthesis of ^{35}S-labeled cRNA probes, and the hybridization and visualization procedures have been previously described in detail (Bondy et al. 1993).

Renal gene expression analysis in adult rats

Microdissection—Male Sprague–Dawley rats (250–300 g) were anesthetized by an intraperitoneal injection of 120 mg/kg body mass of thiobarbitural. After interruption of the aortic blood flow to the kidney, it was perfused with 30 mL cold phosphate-buffered saline (Sigma Chemicals, St. Louis, Missouri, USA) followed by immersion in 30 mL of culture medium [Dubelcco's modified Eagle's Medium (DMEM); Sigma Chemicals] containing 1 mg/mL collagenase (*Clostridium histolyticum*, Sigma Chemicals). The kidney was then removed, cut into slices, and incubated in the DMEM–collagenase solution for 22 min at 37 °C. Microdissection was performed with sharpened forceps at 4 °C under a stereomicroscope. The lengths of dissected segments were determined with an eyepiece micro-meter. In general, 6 to 10 mm of tubule segments were dissected and pooled to constitute one sample. The following specimens were dissected: glomeruli (Glm), proximal straight tubules (PST), proximal convoluted tubules (PCT), medullary thick ascending limb (mTAL), cortical thick ascending limb (cTAL), macula densa containing segment (MDCS), cortical collecting duct (CCD), outer medullary collecting duct (OMCD), inner medullary collecting duct (IMCD). Segments of the proximal convoluted tubule (PCT) may have contained S1 and S2 segments, but not S3 segments. Samples were placed in 100 μL guanidine isothiocyanate buffer (GITC buffer: 4 mol/L guanidine isothiocyanate, 25 mmol/L sodium acetate, 0.8% β-mercatoethanol; pH 6.0), snap frozen in liquid nitrogen, and stored at −80 °C.

RNA isolation—RNA from the renal samples were thawed in ice slurry and sonicated for 15 s. Twenty micrograms of ribosomal RNA from *Escherichia coli* (Boehringer, Minneapolis, Minnesota, USA) was added as the carrier. The 100 μL sample (in GITC

Author Manuscript Author Manuscript Author Manuscript Author Manuscript

buffer) was layered onto a gradient of cesium chloride (100 µL of 97%, 20 µL of 40% cesium chloride in 25 mmol/L sodium acetate buffer) in a 250 µL polycarbonate ultracentrifuge tube. Samples were centrifuged for 2 h at 100 000*g* in a Beckman TLA 100 ultracentrifuge (Beckman Instruments, Fullerton, California, USA) with a fixed angled rotor. The resulting RNA pellet was dissolved in 0.3 mol/L sodium acetate and precipitated with ethanol. The purified RNA was dissolved in diethyl pyrocarbonate treated water containing 20 U RNAsin.

Reverse transcription—Reverse transcription was performed in the presence of 100 IU Moloney murine leukemia virus reverse transcriptase (Superscript BRL, Gaithersburg, Maryland, USA), 0.5 µg oligo$(dT)_{12–18}$ (Pharmacia, Piscataway, New Jersey, USA), 20 IU RNAsin (Promega, Madison, Wisconsin, USA), 10 mmol/L dithiothreitol, 0.5 mmol/L dNTP (Pharmacia), and 1% bovine serum albumin (Boehringer) in the buffer provided by the manufacturer, in an aliquot of 20 µL. Prior to the addition of reverse transcriptase, the reaction mixture was heated to 65 °C for 5 min to allow annealing of the primers. cDNA was synthesized at 42 °C for 1 h and precipitated with 1 µL of linear acrylamide and 4 mol/L ammonium acetate in 100% ethanol. The pellet was redissolved in Tris–EDTA buffer adjusted so that each 2 µL of cDNA corresponded to 1 mm of segment dissected.

Polymerase chain reaction—In each experiment, all tubes were assayed for expression of *Slc23a1* and *Slc23a2*. Rat-specific primers were designed and optimized from the known sequences NM017315 and NM017315, respectively. The following primer pair was chosen and optimized to amplify a 719 bp piece in between base 1021 and base 1740 of the published r-Slc23a1 cDNA open reading frame sequence: sense, 5′-TCATCGAGTCCATCGGTG-3′; antisense, 5′-AGAATCCTCTGAAG ACTG-3′. A 779 bp fragment of r-Slc23a2 was amplified with the sense primer 5′-GACGTCTTCCCTTCCAAC-3′ and the antisense primer 5′-CTTGTTTCCTTTGCTCAC-3′ between bases 1201 and 1980 of the published r-Slc23a2 open reading frame sequence. The primers for both amplifications are located near or in part in the 3′ end of the coding region to ensure optimum detection of the cDNA. Amplification conditions included the following: 0.5 µmol/L of each primer; 50 mmol/L KCL; 10 mmol/L Tris–HCl; 2.5 mmol/L MgCl; 200 µmol/L of dATP, dCTP, and dTTP; 50 µmol/L dGTP; and 150 µmol/L 7-deaza-2′GTP, as well as *Taq* DNA polymerase (Life Technologies). The amplification conditions were as follow: 5 min denaturation at 94 °C followed by 35 cycles of 94 °C for 30 s, 55 for 30 s, and 72 for 30 s. A final extension at 72 °C for 5 min was performed. Amplification products were confirmed by gel electrophoresis and compared with known DNA standards for estimation of the fragment size. The relative intensity of each PCR product band on the ethidium bromide gel was assessed by optical density. The identities of the PCR products were confirmed by sequencing using the dideoxynucleotide chain termination method on an automatic sequencer (ABI PRISM 377, Perkin Elmer, Foster City, Calif.) using the manufacturer's supplies. Sequence data were analyzed using Sequencher 4.1 (Genes Codes Corporation, Ann Arbor, Michigan, USA).

Author Manuscript Author Manuscript Author Manuscript Author Manuscript

Renal gene expression analysis in the developing mouse

We re-analyzed the entire kidney development dataset generated with Affymetrix MOE430 version 2 microarray, which is available for the GenitoUrinary Development Molecular Anatomy Project (GUDMAP.org) (McMahon et al. 2008; Harding et al. 2011). Gene expression data from 54 microarrays were analyzed for the expression of *Slc23a1* after downloading the individual Excel files for different nephron segments at different developmental stages. Data were transformed into relative fluorescent units and graphically displayed. The protocols for the generation of the tissue samples can be found at the GUDMAP protocol web site: http://www.gudmap.org/Research/Protocols. Expression data for the medullary collecting duct, cortical collecting duct and collecting duct distal to the last branch point, S-shaped body, urothelium of the ureter, medullary interstitium, forming muscle layer surrounding the urothelium (ureteral mesenchyme), loop of Henle (including cortical anlage of the loop of Henle and medullary immature loop of Henle), and the proximal tubule were obtained and processed.

Corresponding ISH images were obtained from the GUDMAP web server, the protocols used for tissue isolation, sectioning, in-situ hybridization, and imaging are available at the protocols web site: http://www.gudmap.org/Research/Protocols.

Results

Murine *Slc23a1* is exclusively expressed in the renal proximal tubule

Earliest embryonic *Slc23a1* expression can be detected 14 days post-conception in the developing kidney (Fig. 1A), and emerging gene expression is confirmed in the developing early proximal tubule at embryonic day 15.5 (E15.5, Figs. 1B and 1E). *Slc23a1* is not expressed in the precursors of the early proximal tubule, such as the capping mesenchymal, renal vesicle, and S-shaped body at embryonic day 18 (Fig. 1E). The nephron is derived from capping mesenchymal cells, which undergo a mesenchymal-to-epithelial transition to form the renal vesicle. The cells of the renal vesicle differentiate, elongate, and convolute to form an S-shaped body, from which the glomerulus, proximal tube, loop of Henle, and distal tubule are derived.

In the late stage embryo, at day 18 post-conception, the *Slc23a1* transcript is strongly expressed in the maturing renal cortex, and outside the kidney significant expression can be confirmed in the small intestinal loops and the liver (Fig. 1C). The proximal tubule is the only renal anatomic compartment where *Slc23a1* is expressed in significant amounts in late embryos, starting at day 14 (Fig. 1A) and clearly distinguishable from all other parts of the nephron at day15.5 (Fig. 2A). This expression pattern remains stable in the juvenile and adult kidney (Figs. 2B, 2C, and 2D). In-situ hybridizations of the adult murine kidney shows the *Slc23a1* message in a ray-like pattern beginning at the border of the outer medulla and extending into the renal cortex (Fig. 2D), consistent with a typical proximal tubule anatomic distribution (Chin et al. 1997). This spatial distribution is confirmed by the more sensitive and detailed dark field micrography (Figs. 3A and 3B), and RT–PCR on microdissected nephron compartments (Fig. 3C), mapping *Slc23a1* mRNA expression to the proximal convoluted and straight tubules of the adult murine kidney.

Author Manuscript Author Manuscript Author Manuscript Author Manuscript

Murine *Slc23a2* is uniformly expressed throughout the murine kidney

Slc23a2 mRNA is uniformly expressed throughout the murine late stage embryonic body without signs of defined organ specific patterns (Figs. 4A and 4B) and it does not show a distinct distribution in the adult kidney (Figs. 4C, 4D, and 4E). In renal microdissected segments *Slc23a2* is found in moderate levels, in a relative uniform distribution (Fig. 4F), except that levels are close to the detection limit in the proximal convoluted and straight tubule. This likely indicates a lack of expression in the proximal convoluted and straight tubules, where *Slc23a1* is expressed. Highest *Slc23a2* expression is located in the inner medullary collecting duct, indicating expression by stromal fibroblasts (Chin et al.1997).

Discussion

In this report we resolve the temporal and spatial expression of the *Slc23a1* and *Slc23a2* transcripts in the developing and mature murine kidney. The presented data derived from ISH, microarray, and RT–PCR analysis consistently demonstrate that *Slc23a1* expression is exclusively limited to the proximal tubule during renal development and in the adult kidney. Thus, *Slc23a1* is one of the rare genes displaying extreme component-specific expression (Brunskill et al. 2009). Remarkably, the overwhelming majority of genes with a similar expression pattern encode either known membrane transporters or membrane associated proteins of unknown functions (Brunskill et al. 2009), demonstrating the essential function of the proximal tubule in re-absorption of vitamins and organic compounds/metabolites.

These data of exclusive *Slc23a1* expression in the murine renal proximal convoluted and straight tubules are consistent with the expression pattern reported for the human transcript (Corpe et al. 2010; Eck et al. 2013). This is also consistent with the assumption that gene expression throughout renal development is highly conserved between mammalian species (Thiagarajan et al. 2011). Twenty-five distinct renal cell types are known, which are derived from 2 intermediate mesoderm-derived cell populations: the metanephric mesenchyme and the ureteric bud. The ureteric bud forms a dichotomously branching epithelial tree, giving rise to the cell types that make up the collecting ducts of the kidney and the ureter that connects the kidney with the bladder (Thiagarajan et al. 2011). Before its appearance in the early proximal tubule, *Slc23a1* is not expressed in any precursor tissues, such as the capping mesenchyme surrounding the ureteric bud, which gives rise to the renal vesicle. The renal vesicle then elongates and convolutes to form the S-shaped body, which subsequently gives rise to the glomerulus, proximal tubule, loop of Henle, and distal tubule (Brunskill et al. 2009). *Slc23a1* is not expressed in the ureteric bud derivatives, forming the tip and non-tip sections in the cortex, and the medullary region, to shape the collecting duct system. Expression is also absent in the cortical and medullary interstitium or stroma.

The key role of the ascorbic acid uptake protein Slc23a1 in the maintenance of systemic vitamin C levels was revealed through *Slc23a1*$^{-/-}$ mice (Corpe et al. 2010). For example, female *Slc23a1*$^{-/-}$ mice had an 18-fold increase in fractional excretion of ascorbate in the kidney, and a 70% decrease in circulating vitamin C concentrations compared with the wildtypes. This strongly indicated that Slc23a1 is the only ascorbic acid uptake protein on the apical side of the renal proximal epithelial cell (Corpe et al. 2010; Eck et al. 2013). However, these functional data on *Slc23a1*$^{-/-}$ mice did not rule out the possible disruption

Author Manuscript Author Manuscript Author Manuscript Author Manuscript

of proper kidney development as a contributing factor to renal ascorbic acid losses. The temporal and spatial expression patterns described above clearly identify *Slc23a1*'s sole function in the cellular transport of ascorbic acid, ruling out a function in development, cell adhesion, and cell–cell communication (Brunskill et al. 2009). We therefore rule out a role as an "anlage in statu nascendi" gene, which would be important in the formation of a structure by showing earlier expression in the anlage (Brunskill et al. 2009). The earliest *Slc23a1* expression is detectable in stage IV nephrons, which is the maturing nephron (Thiagarajan et al. 2011), and persists through adulthood. This also confirms that segmentation of the early nephron into proximal, distal, and Loop of Henle elements does not occur until the formation of a stage IV nephron (Thiagarajan et al. 2011). These expression patterns in adult murine are identical to the human site of expression (Eck et al. 2013), allowing an extrapolation to the basic biology of the transporter in humans.

In contrast to the much defined temporal–spatial *Slc23a1* expression in the murine kidney, *Slc23a2* is found in moderate levels and relative uniform distribution pattern, consistent with expression by stromal fibroblasts (Chin et al. 1997). *Slc23a2* is undetectable in the proximal convoluted and straight tubule, ruling out any role in renal ascorbic acid reabsorption, and confirming the notion that Slc23a2 is responsible for ascorbic acid distribution into metabolically active stromal cells (Sotiriou et al. 2002).

Acknowledgements

Mark Levine's contributions were funded through the National Institute of Diabetes and Digestive and Kidney Diseases intramural program grant numbers Z1A DK053218 06 and Z1A DK054506 15. Peter Eck was supported by a Natural Sciences and Engineering Council of Canada (NSERC) Canada Research Chair in Nutrigenomics. Carolyn A. Bondy and Jie Wang (NHLBI) contributed some in-situ hybridization images. Jurgen Schnerman (NIDDK) provided the microdissected nephron samples. This study used data from the GUDMAP database http://www.gudmap.org [microarray and ISH images downloaded in January 2015]. ISH selected from dataset GUDMAP:9176, principal investigator Melissa H. Little, University of Queensland, Brisbane, Australia.

References

Bondy C, Zhou J, and Lee W. 1993. In situ hybridization histochemistry. *In* Handbook of endocrine research techniques. 13th ed. *Edited by* Pablo F and Scanes C. Academic Press, New York. pp. 266–288.

Boyer JC, Campbell CE, Sigurdson WJ, and Kuo SM. 2005. Polarized localization of vitamin C transporters, SVCT1 and SVCT2, in epithelial cells. Biochem. Biophys. Res. Commun. 334(1): 150–156. doi:10.1016/j.bbrc.2005.06.069. [PubMed: 15993839]

Brunskill EW, Aronow BJ, Georgas K, Rumballe B, Valerius MT, Aronow J, et al. 2009. Atlas of gene expression in the developing kidney at microanatomicresolution.Dev.Cell,16(3):482–482.doi:10.1016/j.devcel.2009.02.014.

Chin E, Zamah AM, Landau D, Gronboek H, Flyvbjerg A, LeRoith D, and Bondy CA. 1997. Changes in facilitative glucose transporter messenger ribonucleic acid levels in the diabetic rat kidney. Endocrinology, 138(3): 1267–1275. doi:10.1210/en.138.3.1267. [PubMed: 9048635]

Corpe CP, Tu H, Eck P, Wang J, Faulhaber-Walter R, Schnermann J, et al. 2010. Vitamin C transporter Slc23a1 links renal reabsorption, vitamin C tissue accumulation, and perinatal survival in mice. J. Clin. Invest. 120(4): 1069–1083. doi:10.1172/JCI39191. [PubMed: 20200446]

Daruwala R, Song J, Koh WS, Rumsey SC, and Levine M. 1999. Cloning and functional characterization of the human sodium-dependent vitamin C transporters hSVCT1 and hSVCT2. FEBS Lett. 460(3): 480–484. doi:10.1016/S0014-5793(99)01393-9. [PubMed: 10556521]

Author Manuscript Author Manuscript Author Manuscript Author Manuscript

Eck P, Kwon O, Chen S, Mian O, and Levine M. 2013. The human sodium-dependent ascorbic acid transporters SLC23A1 and SLC23A2 do not mediate ascorbic acid release in the proximal renal epithelial cell. Physiol. Rep. 1(6): e00136. doi:10.1002/phy2.136.

Godoy A, Ormazabal V, Moraga-Cid G, Zúñiga FA, Sotomayor P, Barra V, et al. 2007. Mechanistic insights and functional determinants of the transport cycle of the ascorbic acid transporter SVCT2: activation by sodium and absolute dependence on bivalent cations. J. Biol. Chem. 282(1): 615–624. doi:10.1074/jbc.M608300200. [PubMed: 17012227]

Harding SD, Armit C, Armstrong J, Brennan J, Cheng Y, Haggarty B, et al. 2011. The GUDMAP database — an online resource for genitourinary research. Development, 138(13): 2845–2853. doi:10.1242/dev.063594. [PubMed: 21652655]

Lee JH, Oh CS, Mun GH, Kim JH, Chung YH, Hwang YI, et al. 2006. Immunohistochemical localization of sodium-dependent L-ascorbic acid transporter 1 protein in rat kidney. Histochem. Cell Biol. 126(4): 491–494. doi:10.1007/s00418-006-0186-1. [PubMed: 16673096]

Luo S, Wang Z, Kansara V, Pal D, and Mitra AK. 2008. Activity of a sodium-dependent vitamin C transporter (SVCT) in MDCK-MDR1 cells and mechanism of ascorbate uptake. Int. J. Pharm. 358(1–2): 168–176. doi:10.1016/j.ijpharm.2008.03.002. [PubMed: 18417304]

Maulén NP, Henríquez EA, Kempe S, Cárcamo JG, Schmid-Kotsas A, Bachem M, et al. 2003. Up-regulation and polarized expression of the sodium-ascorbic acid transporter SVCT1 in post-confluent differentiated CaCo-2 cells. J. Biol. Chem. 278(11): 9035–9041. doi:10.1074/jbc.M205119200. [PubMed: 12381735]

McMahon AP, Aronow BJ, Davidson DR, Davies JA, Gaido KW, Grimmond S, et al. 2008. GUDMAP: the genitourinary developmental molecular anatomy project. J. Am. Soc. Nephrol. 19(4): 667–671. doi:10.1681/ASN.2007101078. [PubMed: 18287559]

Nishikimi M, Koshizaka T, Ozawa T, and Yagi K. 1988. Occurrence in humans and guinea pigs of the gene related to their missing enzyme L-gulono-γ-lactone oxidase. Arch. Biochem. Biophys. 267(2): 842–846. doi:10.1016/0003-9861(88)90093-8. [PubMed: 3214183]

Padayatty SJ, Katz A, Wang Y, Eck P, Kwon O, Lee JH, et al. 2003. Vitamin C as an antioxidant: evaluation of its role in disease prevention. J. Am. Coll. Nutr. 22(1): 18–35. doi:10.1080/07315724.2003.10719272. [PubMed: 12569111]

Sotiriou S, Gispert S, Cheng J, Wang Y, Chen A, Hoogstraten-Miller S, et al. 2002. Ascorbic-acid transporter Slc23a1 is essential for vitamin C transport into the brain and for perinatal survival. Nat. Med. 8(5): 514–517. doi:10.1038/0502-514. [PubMed: 11984597]

Thiagaraja RD., Georga KM., Rumball BA., Lesieu E, Chi HS, Taylo D, et al. . 2011. Identification of anchor genes during kidney development defines ontological relationships, molecular subcompartments and regulatory pathways. PLoS One, 6(2): e17286. doi:10.1371/journal.pone.0017286.

Tsukaguchi H, Tokui T, Mackenzie B, Berger UV, Chen XZ, Wang Y, et al. 1999. A family of mammalian Na+-dependent L-ascorbic acid transporters. Nature, 399(6731): 70–75. doi:10.1038/19986. [PubMed: 10331392]

Varma S, Campbell CE, and Kuo SM. 2008. Functional role of conserved transmembrane segment 1 residues in human sodium-dependent vitamin C transporters. Biochemistry, 47(9): 2952–2960. doi:10.1021/bi701666q. [PubMed: 18247577]

Author Manuscript Author Manuscript Author Manuscript Author Manuscript

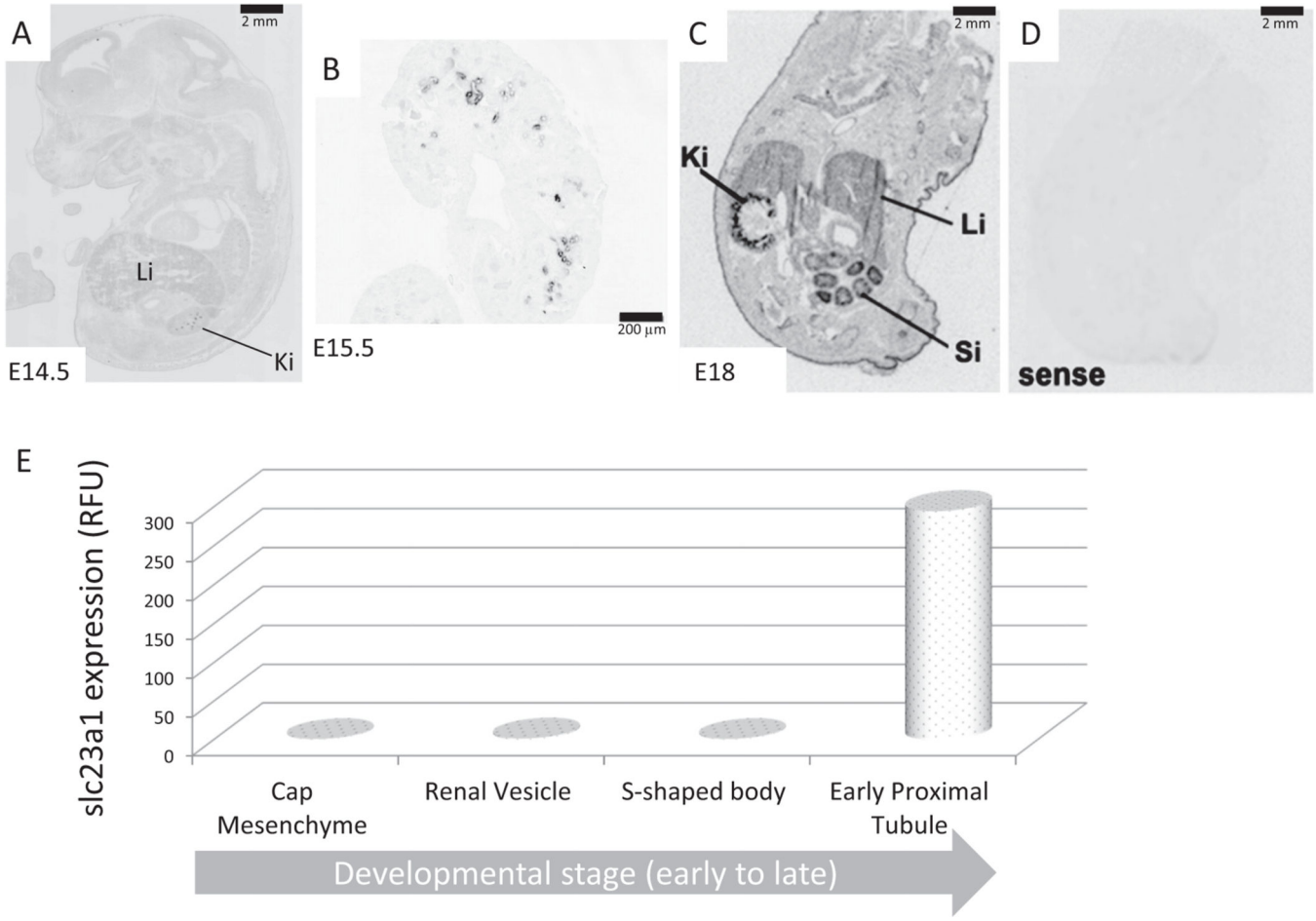

Fig. 1.

Slc23a1 expression in morphological structures of the developing murine and its kidney assed through in situ hybridisation (dark areas indicate expression) and microarray analysis. (A) *Slc23a1* expression in the mouse embryo 14.5 days post-conception (E14.5) emerging in the kidney (Ki). (B) *Slc23a1* expression in kidney of the mouse embryo at 15.5 days post-conception (E15.5). (C) *Slc23a1* expression in the mouse embryo 18 days post-conception (E18) showing well-defined ray-like pattern in the maturing renal cortex (Ki), as well as defined patterns in small intestinal loops (Si) and the liver (Li). (D) Sense *Slc23a1* cRNA hybridized to a slide corresponding with Fig. 1C. (E) Temporal *Slc23a1* expression in developmental precursors of the proximal tubule assessed by microarray analysis and expressed as relative fluorescent units (RFU).

Author Manuscript Author Manuscript Author Manuscript Author Manuscript

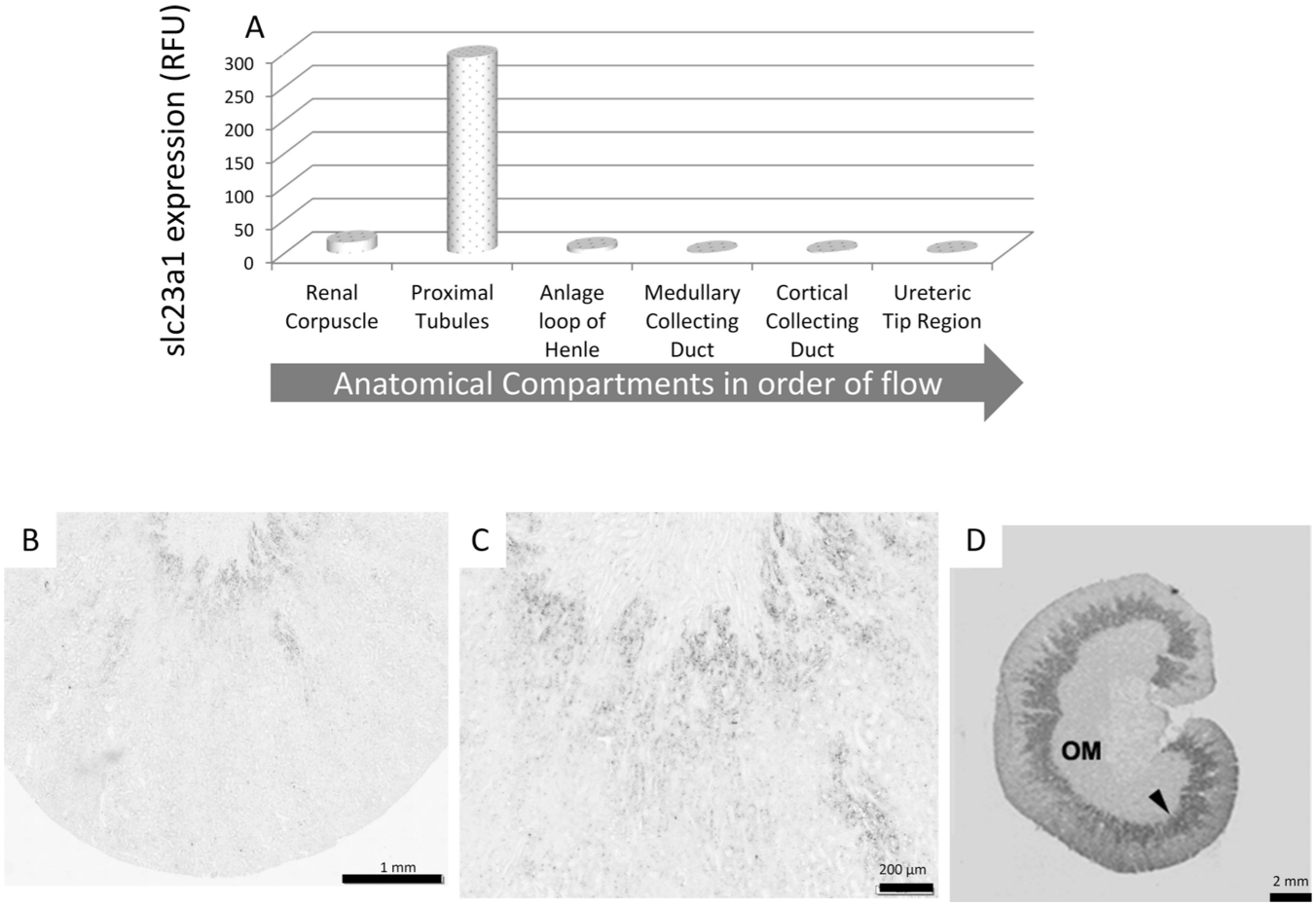

Fig. 2.

Slc23a1 expression in microanatomical compartments of the late embryonic, postpartum, and adult murine kidney assed through microarray analysis and in-situ hybridisation (dark areas indicate expression). (A) *Slc23a1* expression in segments of the embryonal murine nephron at day 15.5 post-conception (E15.5) expressed as relative fluorescent units (RFU) from microarrays. (B and C) *Slc23a1* expression in the kidney of a 7-day-old mouse. (D) *Slc23a1* expression in the adult murine kidney at the border of the outer medulla (OM).

Author Manuscript Author Manuscript Author Manuscript Author Manuscript

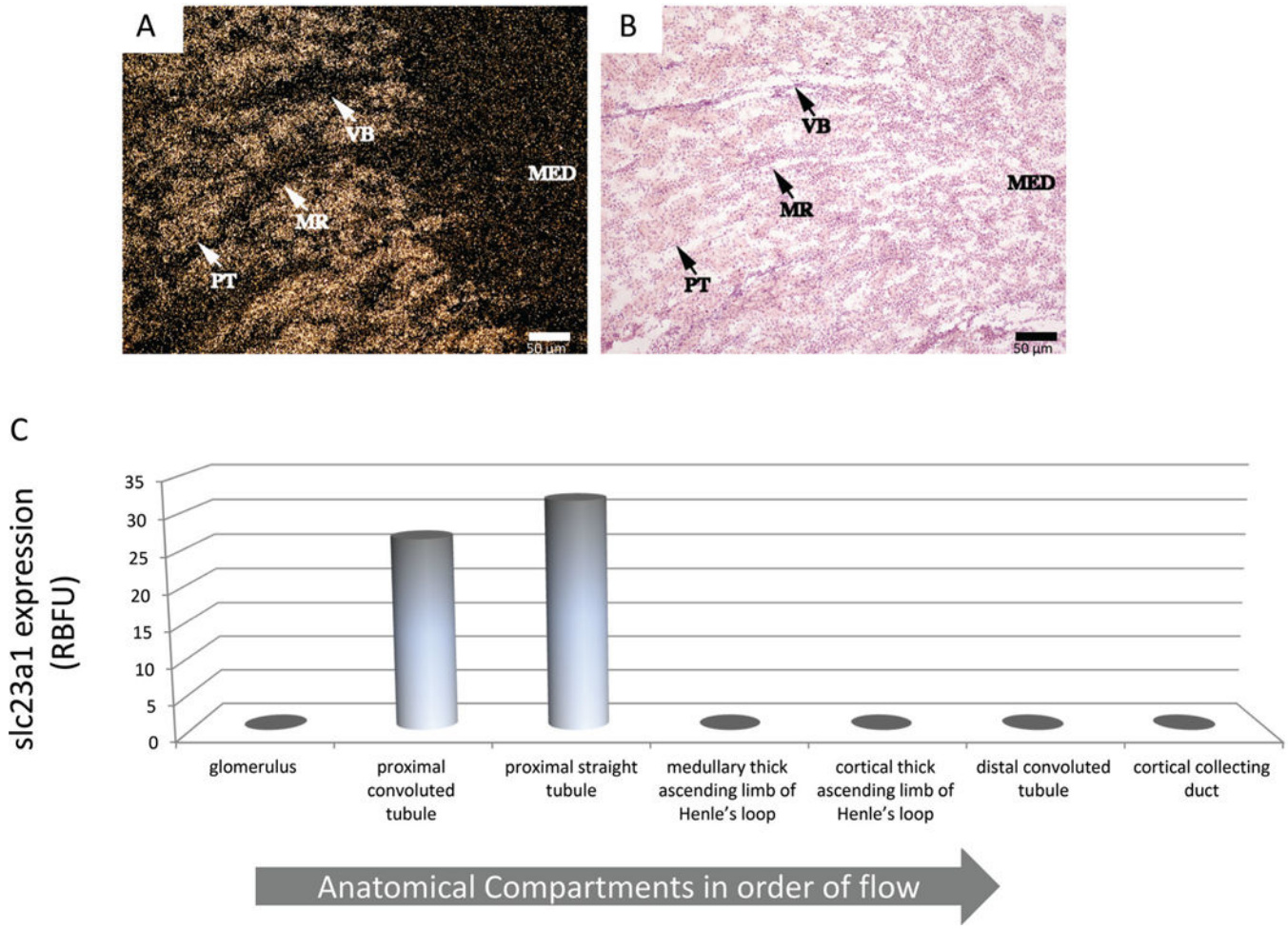

Fig. 3.

Slc23a1 expression in microanatomical compartments of the adult murine kidney. (A) *Slc23a1* expression in the adult murine kidney using a dark field micrograph shows expression in proximal tubules (PT, light spots), but no signal in vascular bundles (VB, dark areas) or the ascending thick limbs of Henle localized in the medullary rays (MR, dark areas). (B) Haematoxylin and eosin stained bright-field image corresponding to image 3A. Here, PT, VB, and MR were microscopically identified by a pathologist. (C) *Slc23a1* expression in dissected nephron segments from the adult murine kidney assessed with quantitative PCR expressed as relative band fluorescent units (RBFU).

Author Manuscript Author Manuscript Author Manuscript Author Manuscript

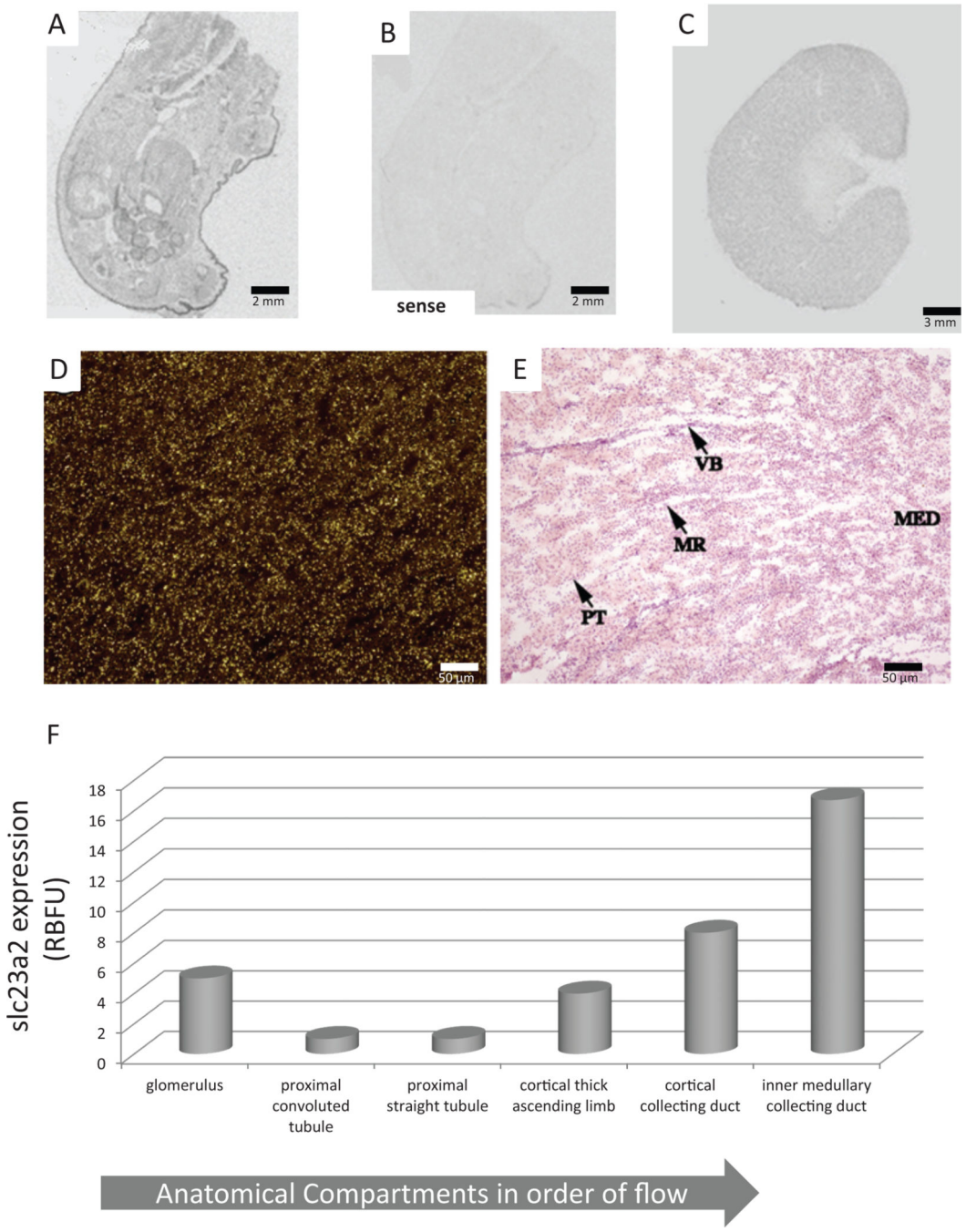

Fig. 4.

Slc23a2 expression in the murine kidney assessed by in-situ hybridization (A, B, and C), dark-field micrographs (D and E), and quantitative PCR (F). (A) *Slc23a2* expression in the mouse embryo at day 18 (E18). (B) Corresponding image to Fig. 4A hybridized with sense RNA. (C) *Slc23a2* expression in the adult murine kidney. (D) *Slc23a2* expression in the adult murine kidney using a dark-field micrograph shows relatively uniform expression. (E) Haematoxylin and eosin stained bright-field image corresponding to image 4D. Here, PT, VB and MR were microscopically identified by a pathologist. (F) *Slc23a2* expression in

Author Manuscript Author Manuscript Author Manuscript Author Manuscript

dissected nephron segments from the adult murine kidney assessed with quantitative PCR expressed as relative band fluorescent units (RBFU).